Journal of Maps

ISSN: (Print) (Online) Journal homepage: https://www.tandfonline.com/loi/tjom20

Deep-seated gravitational slope deformations in central Sardinia: insights into the geomorphological evolution

Valentino Demurtas, Paolo E. Orrù & Giacomo Deiana

To cite this article: Valentino Demurtas, Paolo E. Orrù & Giacomo Deiana (2021) Deep-seated gravitational slope deformations in central Sardinia: insights into the geomorphological evolution, Journal of Maps, 17:2, 594-607, DOI: 10.1080/17445647.2021.1986157

To link to this article: https://doi.org/10.1080/17445647.2021.1986157

JOURNAL OF MAPS
2021, VOL. 17, NO. 2, 594–607
https://doi.org/10.1080/17445647.2021.1986157

SCIENCE

OPEN ACCESS Check for updates

Deep-seated gravitational slope deformations in central Sardinia: insights into the geomorphological evolution

Valentino Demurtas, Paolo E. Orrù and Giacomo Deiana

Department of Chemical and Geological Sciences, University of Cagliari, Monserrato, Italy

ABSTRACT
In this study, we analyse deep-seated gravitational slope deformations (DSGSDs) in central Sardinia. The area is characterised by plateaus with a prominent limestone scarp overlying metamorphites. A comprehensive mapping of structural, karst, fluvial, and slope morphologies in Pardu and Ulassai valleys is presented herein. The uplift linked to the Plio-Pleistocene tectonic activity leads to high-slope topography, which favours gravitational processes, such as DSGSDs and rock-avalanches. Although DSGSD is a common phenomenon in the relief of the central Mediterranean region, it has never been studied in Sardinia. We describe the kinematic models and geomorphological evolution of DSGSD in Sardinia for the first time. The application of light detection and ranging, high-resolution unmanned aerial vehicle photogrammetry, and geological, structural, and geomorphological surveys enabled a depth morphometric analysis and the development of interpretative three-dimensional models. The geo-structural setting and high relief energy associated with recent upliftment are the major controlling factors of DSGSDs.

ARTICLE HISTORY
Received 24 May 2021
Revised 23 August 2021
Accepted 23 September 2021

KEYWORDS
Deep-seated gravitational slope deformation; tectonic geomorphology; morphostratigraphy; geomorphological mapping; rock avalanche; UAV

1. Introduction

Deep-seated gravitational slope deformation (DSGSD; Dramis & Sorriso-Valvo, 1994) is a complex type of rock slope failure characterised by large dimensions generated in stone rocks (Dramis et al., 2002). DSGSDs are characterised by slow movements that can suddenly accelerate and cause catastrophic collapse of large sections of the deformed slopes (Agliardi et al., 2020; Crosta & Agliardi, 2003; Nemčok, 1972; Ostermann & Sanders, 2017; Radbruch-Hall, 1978). Therefore, this phenomenon represents a major geological hazard associated with the deformation of large infrastructures and the generation of secondary landslides. Although DSGSDs represent a major geological hazard, information about them is scarce so far (Soldati, 2013). Advanced technologies in both remote sensing (e.g. satellite data and space-borne interferometric synthetic aperture radar) (Frattini et al., 2018; Mantovani et al., 2016; Novellino et al., 2021) and proximal sensing such as unmanned aerial vehicle (UAV; Deiana et al., 2021; Devoto et al., 2020; Eker & Aydın, 2021) and light detection and ranging (LiDAR) have enabled a better understanding of these processes. They are characterised by extremely slow deformation rates (Cruden & Varnes, 1996) and landform assemblages such as double-crested ridges, trenches, synthetic and antithetic (uphill-facing) scarps, tension cracks, and convex (bulged toes) and deep basal shear zones (Agliardi et al., 2001; Chigira, 1992; Crosta et al., 2013; Mariani & Zerboni, 2020; Panek & Klimeš, 2016). Shear zones exhibit the characteristics of cataclastic breccias with abundant fine matrix (Crosta & Zanchi, 2000) and thicknesses up to tens of metres (Ostermann & Sanders, 2017).

In this study, we present three cases of DSGSDs in Sardinia. The study area is located in Ogliastra (central-east Sardinia) in the Pardu River Valley (Figure 1). The area is characterised by wide plateaus, called Tacchi, with a prominent Jurassic limestone scarp overlying Palaeozoic metamorphites (Carmignani et al., 2016; Pertusati et al., 2002).

The major evidence of DSGSDs in the Pardu River Valley is the presence of large prismatic blocks of dolomitic Mesozoic slab displaced up to tens of metres downstream from the initial altitude. The geomorphological features associated with DSGSDs vary along the slope. A set of ridge-top trenches, with widths up to 50 m, lengths of hundreds of metres, and depths of >50 m is present in the plateau edge. The middle slopes are characterised by tilted blocks, shear zones, and rockfall deposits. Large block deposits with rock avalanche features in the foot-slope are associated with the final-collapse phases of the DSGSDs.

For the first time in this setting, we delineated long-term deformations, such as gravitational slides

CONTACT Valentino Demurtas valentino.demurtas@unica.it Department of Chemical and Geological Sciences, University of Cagliari, Monserrato 09042, Italy

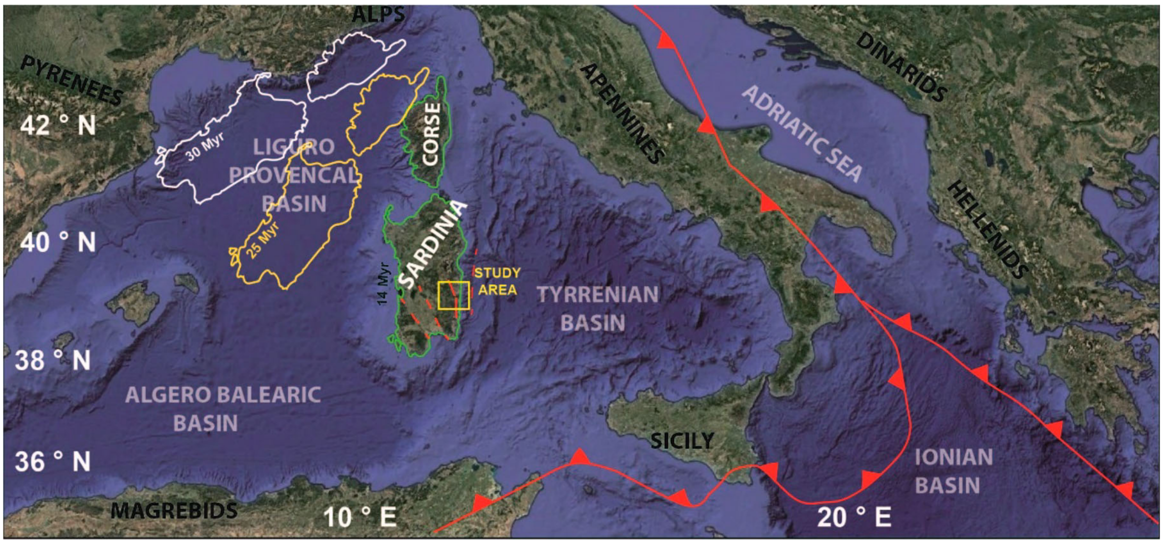

Figure 1. Geographical location and structural features of the study area modified after Deiana et al. (2021): red lines represent thrust fronts; white lines are the Sardinian–Corse Block translation 30 Ma; yellow line represents the Sardinian–Corse Block translation 25 Ma (modified after Carminati & Doglioni, 2005); green line represents the Sardinian–Corse Block translation 14 Ma (Gattacceca et al., 2007).

(Zaruba & Mencl, 1982) with lateral spreading (Cruden & Varnes, 1996; Jahn, 1964; Pasuto & Soldati, 1996) and sackung kinematics (Bisci et al., 1996; Radbruch-Hall, 1978; Radbruch-Hall et al., 1976; Zischinsky, 1966, 1969), which involve giant carbonate blocks, and the underlying foliated metamorphites. Geomorphological and geological analyses enabled the identification of various evolutionary stages as follows: (I) early stage represented by the spreading at the plateau edges, (II) second stage of the old DSGSDs located in the middle slope, and (III) third stage corresponding to the final evolution of the deformation process developed through collapse.

We highlight the occurrence of DSGSDs associated with the evolution of river slope in the uplift setting within the low seismic and low tectonic activity regions of Sardinia. Thus, we analysed the geomorphological evolution of the slope, particularly focusing on the probable and catastrophic evolution of these processes in an urban setting.

A geomorphological map at a scale of 1:10.000 was generated showing: (i) the karst morphology on carbonate plateaus; (ii) the gravity feature on the edge plateau linked to the extensional trenches and tilted blocks; (iii) different landslide deposits on the slopes (rockfalls, palaeo-DSGSDs, slope debris, and rock avalanches); and (iv) hydrographic elements (e.g. creeks, canals, and fluvial elbows).

1.1. Geological setting

East-central Sardinia (Italy) is characterised by a Jurassic dolomitic plateau (Tacchi) overlying a metamorphic Palaeozoic basement, primarily comprising metasandstone, quartzites, and phyllites (Figure 2) (Carmignani et al., 2016; Pertusati et al., 2002).

The area is characterised by the Pardu River Valley in the east and the Barigau River Valley in the south-west; the central and north-western sectors include extensive dolomitic plateau called Tacco of Ulassai. The geological basement comprises Palaeozoic metamorphites affected by complex plicative structures and regional low-grade metamorphism (Carmignani et al., 2001, 1994; Elter et al., 2004, 2010). The major Palaeozoic units are the Filladi Grigie del Gennargentu Formation and Monte Santa Vittoria Formation, which constitute metarenites, quartzites, shales, and metavolcanites (Middle Cambrian–Middle Ordovician) (Meloni et al., 2017; Pertusati et al., 2002; Vai & Cocozza, 1974). The metamorphic basement summit has suffered chemical alteration associated with a warm humid climate during the Permian and Triassic periods (Costamagna & Barca, 2004; Marini, 1984).

An angular unconformity of Mesozoic sedimentary succession rests on the metamorphic basement. Basal layers are primarily fluvial sediments of the Genna Selole Formation (Middle Jurassic), which are overlain by dolomitic limestones of the Dorgali Formation (Middle–Upper Jurassic). (Costamagna et al., 2018; Costamagna & Barca, 2004; Dieni et al., 1983; Pertusati et al., 2002). These Mesozoic deposits are extensive and decipherable from their plateau morphology. The Genna Selole Formation (Costamagna, 2015; Dieni et al., 1983) represents a mixed succession of siliciclastic to siliciclastic–carbonate deposits. The Dorgali Formation is represented by dolomitic sequences with thickness up to tens of metres. The lower part, with a thickness of approximately 30 m, is affected by marl intercalations, whereas the upper part is typically

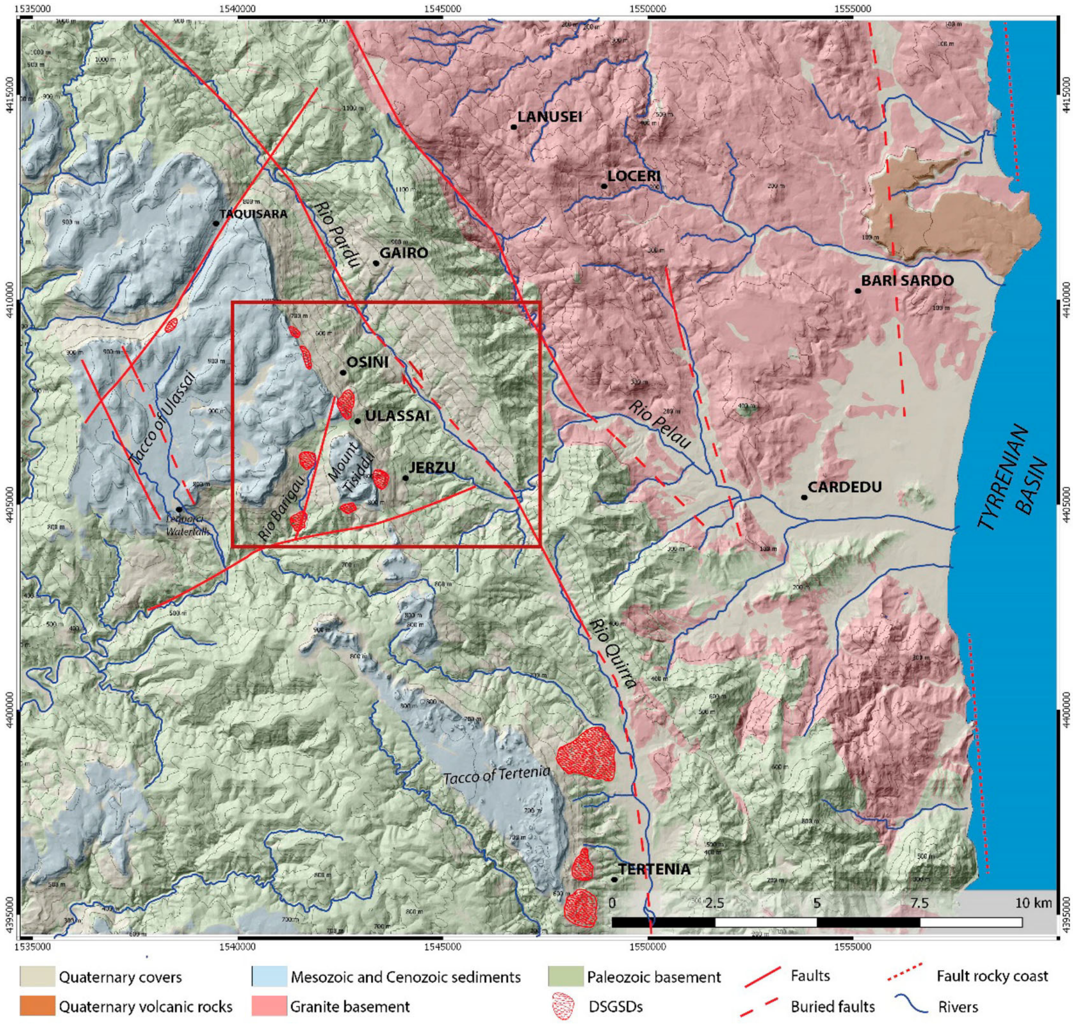

Figure 2. Geolithological sketch map of the study area based on geological data of Autonomous Region of Sardinia. The red boxes indicate the location of the main map that covers Pardu Valley and the east side of Tacco of Ulassai.

massive. Mesozoic units are sub-horizontal strata with an attitude of approximately N90/0–5°, and the plateau edges can reach a dip amount of up to 40° and direction parallel to the slope owing to the DSGSD.

Quaternary covers, represented by continental deposits, are primarily colluvial and alluvial deposits. The most extensive outcrops represent landslide deposits, including rockfalls, toppling, and collapsed DSGSDs at the foot-slope of the Tacchi, abundant on the right slopes of the Pardu and Barigau rivers. Moreover, terraced alluvial deposits have also been identified in the downslope.

The rockfalls and toppling landslides have been characterised by different sedimentological features based on age. These deposits are associated with rockfalls affecting the plateau edge wall and the collapse of some parts of the DSGSDs.

1.2. Tectonic and geodynamic settings

The geodynamic setting is associated with the collisional dynamics between the African and European plates (Figure 1). The structural setting is associated with the Alpine cycle, which first appeared with a strike-slip fault in the Oligo–Miocene and in the Pliocene and Quaternary with an extensional component (Carmignani et al., 2001, 2016; Carminati & Doglioni, 2005; Cherchi & Montadert, 1982; Gattacceca et al., 2007; Gueguen et al., 1997; Oggiano et al., 2009; Ulzega et al., 2002).

The major features in the study area are the NW–SE faults on which the Pardu Valley is engraved, and the secondary fault directions include ENE–WSW and NNE–SSW (Pertusati et al., 2002).

The Plio-Quaternary tectonic phase is associated with conspicuous N–S faults (Casula et al., 2001). These rectilinear and normal faults are also evident in the continental margin and control its morphology (Figure 2). In the continental region, these N–S faults are associated with alkaline basalts with an age of approximately 3.9 Ma (Lustrino et al., 2007). Quirra River follows this N–S direction from the south of the Pardu River capturing elbows and flows in a straight line for approximately 30 km (Figure 3).

Based on preliminary geodetic data from the Peri-Tyrrhenian Geodetic Array network, Ferranti et al.

(2008) revealed the presence of low internal deformation in Sardinia. In Sardinia, seismicity is typically scattered and sporadic, except for the dozen tremors detected following the ML4.7 earthquake of 7 July 2011 in the Corsican Sea, which primarily characterises the edges of the continental lithosphere block. Significant seismic events also occurred in the eastern sector, in particular, three events with a magnitude > 4 (26 April 2000, magnitude ML 4.2 and 4.7, and 18 December 2004, magnitude ML 4.3) located in the central Tyrrhenian Sea approximately 60 km east of Olbia in the Comino depression (Cimini et al., 2016). The most recent low-magnitude earthquake events were ML 1.8 (Escalaplano, 4 April 2019) and ML 1.6 (Perdasdefogu, 14 October 2020) (INGV, 2021).

1.3. Geomorphological setting

The landscape is characterised by sub-horizontal carbonate plateaus, separated by deep rectilinear valleys engraved in the Palaeozoic basement for several hundreds of metres (Maxia et al., 1973; Ulzega & Marini, 1973). Erosion primarily acted on the Oligo–Miocene strike-slip faults with an increase in the erosive rate during the Plio-Pleistocene uplift phases (Marini & Ulzega, 1977). A significant karstic process has acted on plateau surfaces, comprising ancient palaeoforms and currently hypogeal and superficial morphologies (De Waele et al., 2005, 2012). Karst palaeoforms represented by complex cockpit doline types have been characterised in the area in a humid and warm morphoclimatic setting (Fleurant et al., 2008; Liang & Xu, 2014; Waltham, 2008). These dolines are separated by residual reliefs called Fengcong, sorted along the major structural features. The hypogean karst enabled the development of sinkholes, karst springs, cavities, and caves (e.g. Su Marmuri Cave and Is lianas Cave). The combined action of karst, uplift, river erosion, and gravity has led to the formation and evolution of numerous hanging valleys on the plateau surface (Ulzega & Marini, 1973).

The presence of major regional faults has influenced the watercourses, which maintain a prevalent N–S direction in the Pardu River (set on the main fault), toward the western side of the map, corresponding with the secondary faults. Considering the descriptive parameters, geometrical conditions, and longitudinal profile, the evolutionary conditions of the Pardu Valley are associated with a cycle of underdeveloped fluvial erosion, suggesting a relatively young age of engraving (Marini & Ulzega, 1977; Maxia et al., 1973; Ulzega & Marini, 1973).

The evolution of Pardu River is closely associated with that of Quirra River (Palomba & Ulazega, 1984; Pertusati et al., 2002). Pardu River flows from the NW toward the SE and then abruptly changes direction toward the NE. At this point, a capture elbow adjacent to the present head of the Quirra River is well developed. The upstream part of Quirra River flows at an altitude of approximately 200 m higher than the Pardu River.

It also presents an over-sized and over-flooded valley with respect to the upstream catchment area. Moreover, there are various orders of terraces and deposits in the Pleistocene. This setting indicates that the Pardu River, previously flowing south along with the Quirra River, was captured by Pelau River (De Waele et al., 2012; Palomba & Ulzega, 1984).

Gravity-related mass movements occur along carbonate cornices with rockfalls and toppling. We have focussed on the DSGSDs in this study, as they are important in the morphological evolution of the carbonate plateau.

2. Methods

Geological and geomorphological analyses were performed and a 1:10.000 geomorphological map was generated in accordance with cartographic models in the literature related to geomorphological mapping (GNGFG, 1994; ISPRA 2007; ISPRA & AIGEO, 2018; Miccadei et al., 2012; Smith et al., 2011). A remote sensing survey, accompanied by the interpretation of aerial photos and digital terrain models (LiDAR data of 1-m cell size, by Autonomous Region of Sardinia acquired in 2008), and field surveys were performed to analyse vast areas, including the Tacco di Ulassai and the Pardu River and Barigau River valleys.

The main map was created using the ESRI ArcGIS/ArcMap using the Regional Technical Cartography of the Autonomous Region of Sardinia at 1:10.000 scale. We comprehensively analysed three areas with specifically interesting DSGSD process: Bruncu pranedda, Scala San Giorgio, and Tisiddu Mountain (Figure 3).

To analyse the DSGSDs at the local scale, we used high-resolution digital elevation models (DEMs) acquired via structure for motion from a UAV. Structural and geomorphological field mapping surveys were performed at a 1:200 scale for each landslide, thereby enabling the creation of a geological 3D model of the slope deformations (Clapuyt et al., 2016; Eker & Aydın, 2021; Peternal et al., 2017; Valkaniotis et al., 2018). Briefly, 100 structural survey stations were set in the metamorphic basement and in the Mesozoic units using geological compass. Structural data were processed using Rocscince Dips.

The aerial surveys were performed using UAVs (DJI Phantom 4) flying at altitudes of 50–60 m above ground level. The acquired images were analysed and processed using photogrammetric Agisoft MetaShape software and constrained by 10–12 ground control points using GEODETIC LEICA GNSS for each area. The resulting orthorectified mosaic and DEM (WGS 84 datum and UTM 32N projection) had a cell size of

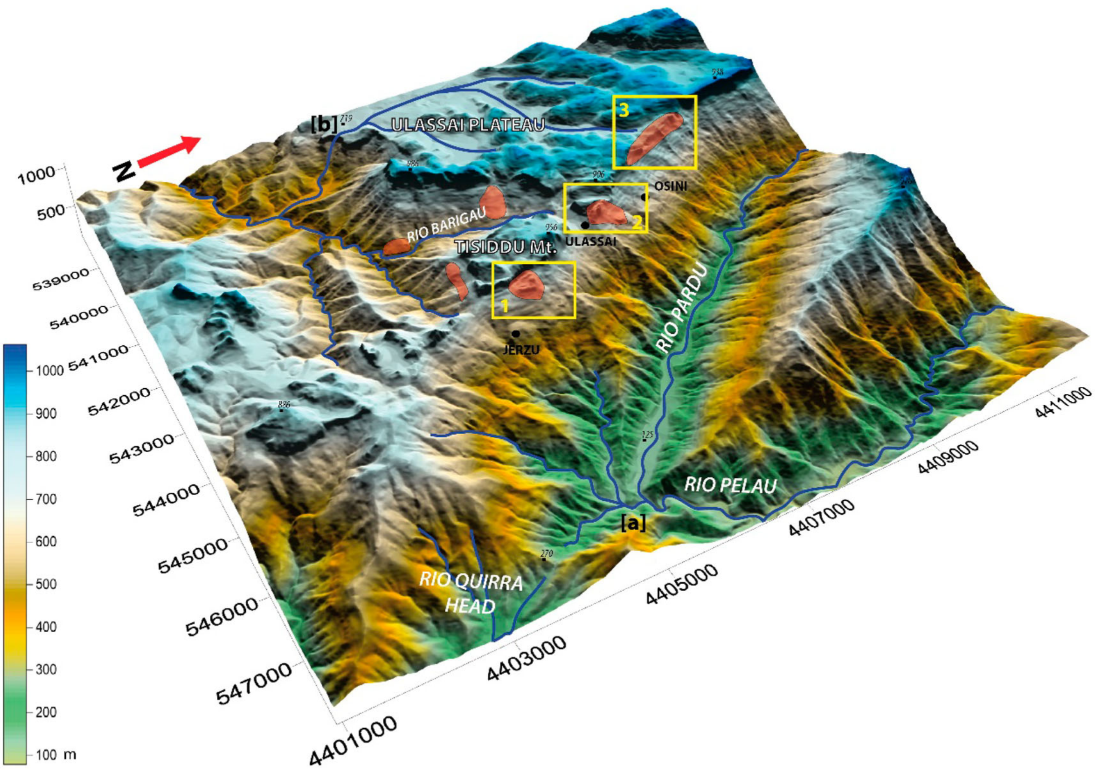

Figure 3. Three-dimensional (3D) model of Pardu River (Rio Pardu) Valley and Ulassai Plateau. Blue lines represent major hydrographic features, and red areas represent the major DSGSDs. (a) Fluvial capture elbow; (b) Lequarci waterfall. (1) Tisiddu Mountain DSGSD; (2) Bruncu Pranedda DSGSD; (3) Scala San Giorgio DSGSD.

5 cm/pixel and were considered sufficiently precise to be used for the geomorphological analysis. 3D high-resolution UAV models were used to develop interpretative superficial models using geomorphological evidence and stratigraphic and structural data of the DSGSDs. Geological interpretative cross-sections of geologic features crossing the major DSGSDs were also generated to define the movement kinematics, deformative style, and deep geometries of the DSGSDs.

3. Results

3.1. Geomorphological map

The cartographic synthesis was based on the lithologies on which landforms were highlighted, with distinct morphogenetic processes and relative chronological positions.

Geomorphological map shows the lithology from the Palaeozoic basement to the continental Quaternary covers (Figure 4).

The major physiographic units presented in the geomorphological map are the Tacco of Ulassai, Tisiddu Mountain, and the two main valleys, namely Pardu River and Barigau River valleys. The Ulassai Plateau, which comprises Mesozoic dolomitic lithologies, is affected by various superficial and underground karst morphologies (De Waele et al., 2012). A karst palaeo-landscape with a sub-tropical climate consisting of cockpit and Fengcong was detected (Fleurant et al., 2008). The latter, characterised by gentle relief, is aligned in the direction of the Oligo–Miocene faults. These formations are the major pathways of underground waterflows, on which sinkholes have developed. The plateau surface is affected by extensive polje-type dolines, which defines an extensive hydrography. The catchment area of the plateau flows out of the Santa Barbara area, which flows into the Ulassai stream after an 80-m hydraulic jump (Lequarci waterfall) (Figure 3).

The edge of the plateau was affected by gravitational processes at different scales. Moreover, there widespread rockfalls and toppling of various magnitudes were present. Three orders of landslide deposits were identified, namely cemented, quiescent, and active.

The valley floor of the Pardu River in the upper part is characterised by a bed set on rock with major erosive features, whereas in the downstream part near the capture elbow, alluvial deposits exist with two orders of terraces. Downstream of the capture, the river resumes the erosive character with the valley floor set on the rock.

The legend signifying geomorphology in this study was conceived to effectively represent the features of the study area. We highlighted outcropping bedrock lithology, tectonic features, superficial deposits, and the distribution of structural, gravitational, and karst landforms.

3.2. Morphostructural setting of DSGSDs

Various areas affected by DSGSDs located at the edges of the carbonate plateau were identified, with

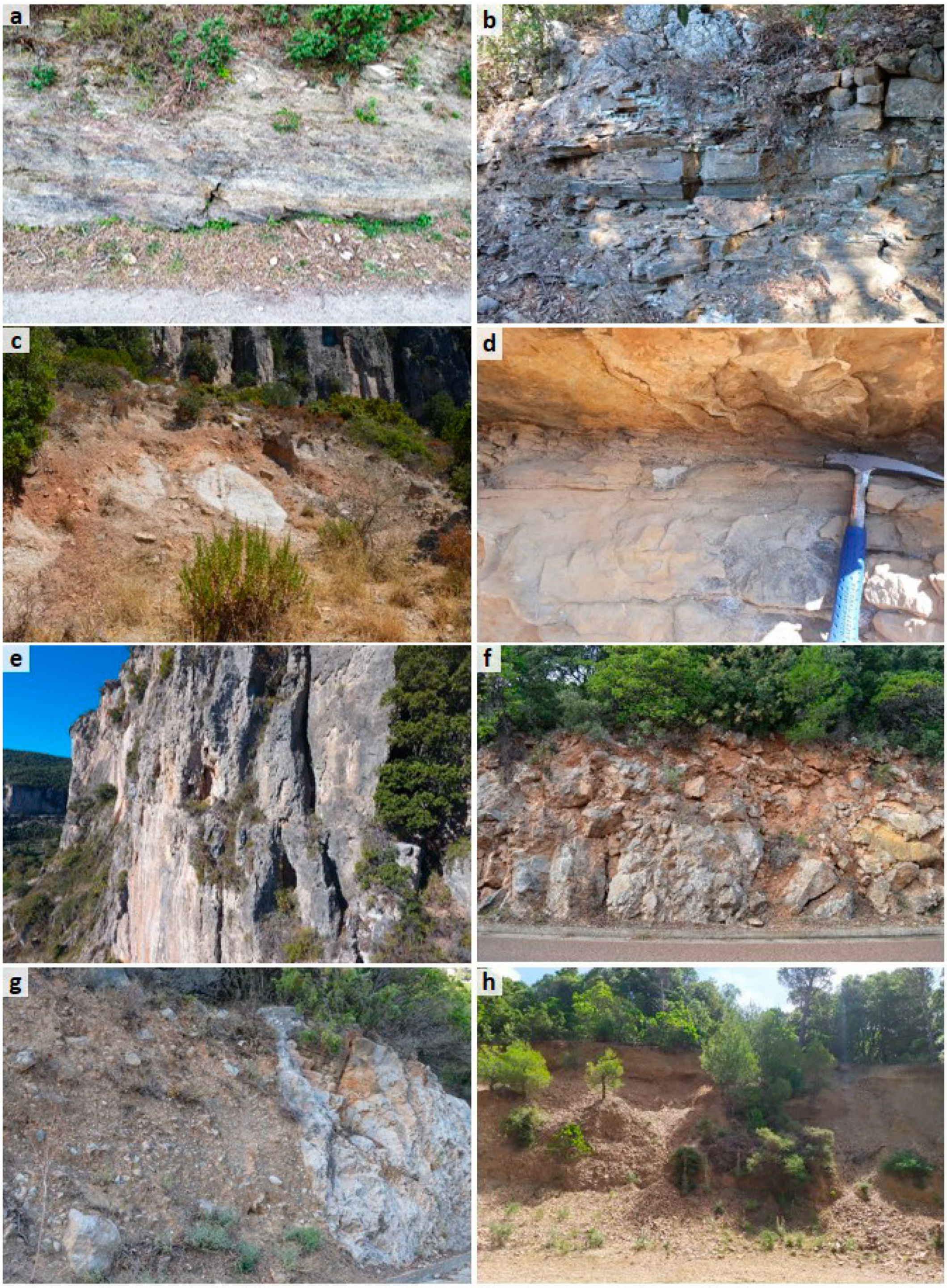

Figure 4. Major geological units presented in the main map: Metamorphic basement: (a) altered phyllites; (b) Fractured metasandstone and quartzites. Transitional and marine Mesozoic succession: (c) Genna Selole Formation (siliciclastic–carbonate deposits and clays); (d) Basal facies of Dorgali Formation (layered dolostone and marls); (e) Dolostone of massive Dorgali Formation. Rockfall deposits: (f) Cemented; (g) Quiescent; (h) Slope deposits.

the major ones located on the east side of Tacco di Ulassai and Tisiddu Mountain. The main structures that indicate the deep gravity phenomenon were large and deep extensional trenches which are evident in the carbonate lithotypes. A complex structural setting was deciphered based on the analysis of faults, foliation, and tectonic-gravitational structures (Figure 5). Trenches had lengths of several hundreds of metres and a decametric opening and depth (Figure 6).

The Bruncu Pranedda DSGSD depicted two regions with different settings located in the top and middle slopes. In the top slope toward the east of the largest extensional trenches called Pranedda Canyon (Figure 6(A1–A3); Figure 7(A,A1,D)), the rock mass fracturing increased, and the attitude of the Dorgali Formation is toward the east, with a dip amount of up to 40°. In this area, both facies of the Dorgali Formation were visible, with the summit comprising dolomitic banks and the lower part characterised by an alternation of well-stratified dolomites and marls. This subdivision was not observed in the middle slope (Figure 6(A4)), where basal marly levels do not appear on the surface. This indicates that the basal facies (approximately 30 m) were partially covered by slope deposits; however, they also sank a few metres inside the fractured and altered Palaeozoic metamorphic basement. This can be correlated with the field observations at the same altitude, with the basement and the massive facies of the Dorgali Formation.

The Scala San Giorgio DSGSD is located north of Osini Village (Figures 6(B) and 7(C)) and is characterised by two major extensional trenches parallel to the slope that affect the Dorgali Formation with dip amount up to 20°. All the sequences of the Dorgali Formation are exposed; however, the Genna Selole Formation is covered by rockfall deposits.

The Tisiddu Mountain DSGSD in the south of Ulassai Village is characterised by a highly fractured segment of the Dorgali Formation located tens of metres downstream. Only the top massive banks of dolostones are visible. The basal level was partially sinking in the metamorphic basement.

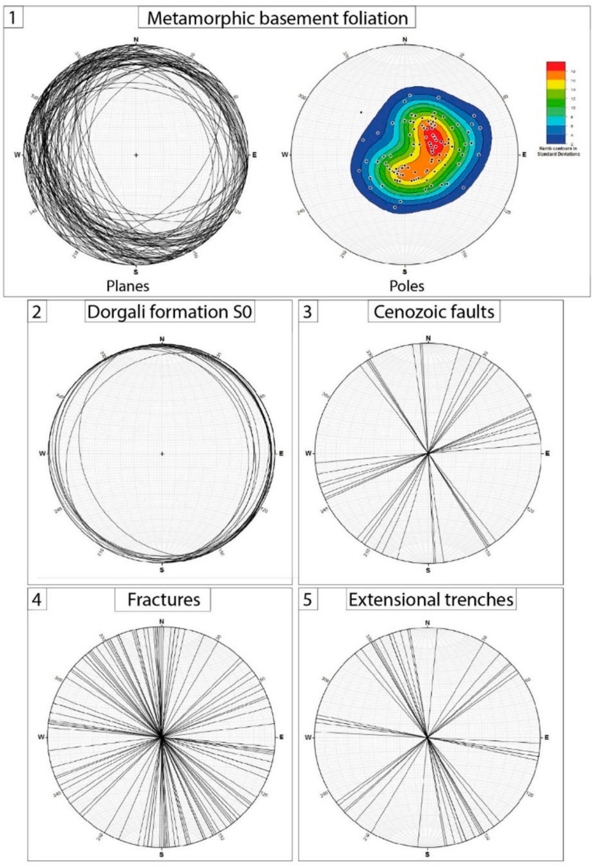

Figure 5. Stereographic projections of tectonic and gravitational structures. (1) Low-angle dip schistosity in the metamorphic basement; (2) Dorgali Formation layering. The larger angles indicate the blocks of the DSGSD; (3) Primary Cenozoic faults, NW–SE and secondary sub-vertical faults; (4) Vertical fractures in the Mesozoic units associated with the tectonic structures; (5) Extensional trenches.

Shear zones are located in different geological units that represent structural weaknesses (Figure 8).

(I) The top of the metamorphites was affected by sub-horizontal foliation (Figure 5) and advanced weathering, and the rock exhibited a reddish or whitish colour. This type of alteration could be linked to the pre-transgressive Mesozoic period (Marini, 1984); (II) Genna Selole Formation exhibited plastic clay layers; (III) basal levels of Dorgali Formation were characterised by the alternations of marl and dolomite.

Geomorphological evidence and stratigraphic and structural analyses enabled the identification of various DSGSDs characterised by different kinematics. From the structural analysis (Figure 5), the major faults with NW–SE and NE–SW directions were in concordance with the main trenches. The secondary trenches and the joints did not exhibit a good correlation with the large-scale structures because they were associated with the features inside the deformation rock mass. Lateral spreads were developed at the plateau edge due to the sub-vertical pre-existing fractures (Figure 5). Consequently, there was a predominant horizontal movement associated with vertical fractures in the carbonate and a zone of ductile basal deformation that affected the Genna Selole Formation and the summit, which altered the metamorphites (Bruncu Pranedda top slope and San Giorgio DSGSD). DSGSDs with a higher vertical shift represented a more advanced stage with sackung features (Tisiddu Mountain and middle slope of Bruncu Pranedda). A large part of the deformation affected the Palaeozoic basement, which was evidenced by the sinking of the carbonate sequence in the metamorphites.

These DSGSs were associated with numerous rockfalls and toppling landslides that affect carbonate walls. Dolomitic blocks with sizes up to 30 m on each side were identified, moving up to 900 m away from the detachment points, which were linked to mega-rockfall events with rock avalanche features (Figure 6(D)). We also identified mega-blocks of Dorgali Formation in the downslope that were associated with collapsed palaeo-DSGSD.

4. Discussion

Geomorphological data regarding the DSGSD of Bruncu Pranedda, Scala San Giorgio, and Tisiddu Mountain were used to generate geological sections for reconstructing a hypothetical surface of basal rupture and deep geometries (Figure 8).

Geological and geomorphological analyses using high-resolution topographic data enabled the identification of different DSGSD kinematic and evolutionary models. Based on the collected data, it was possible to identify three evolutionary stages.

The initial movement stage was characterised by lateral spread kinematics (Delgado et al., 2011; Dramis

Figure 6. UAV images of the DSGSD showing the major geomorphological and structural features. The white dashed lines represent the major extensional trenches. (A1). Panoramic view of the Ulassai Village. (A2) Bruncu Pranedda DSGSD. (A3) Top slope sector. (A4) Middle slope sector. (B) San Giorgio DSGSD. (C) Tisiddu Mountain DSGSD. (D) Evidence of collapse deposits of rock avalanches. Recent collapse near Ulassai Village. (D1, D2) Palaeo-collapses of mega-blocks, 20–40 m for each side.

& Sorriso-Valvo, 1994; Fioraso, 2017; Gutiérrez-Santolalla et al., 2005; Pánek & Klimeš, 2016; Taramelli & Melelli, 2008) (Figure 8(1,2a)), with a separation of the DSGSD from the edge of the plateau. This occurred via horizontal movement without vertical sinking.

The stratigraphic setting is characteristic of the lateral spreads because the Dorgali Formation (hard formation) rests on the Genna Selole clays and on an altered and fractured schist basement (plastic formations). In the carbonate lithologies, the deformation is brittle and develops with a

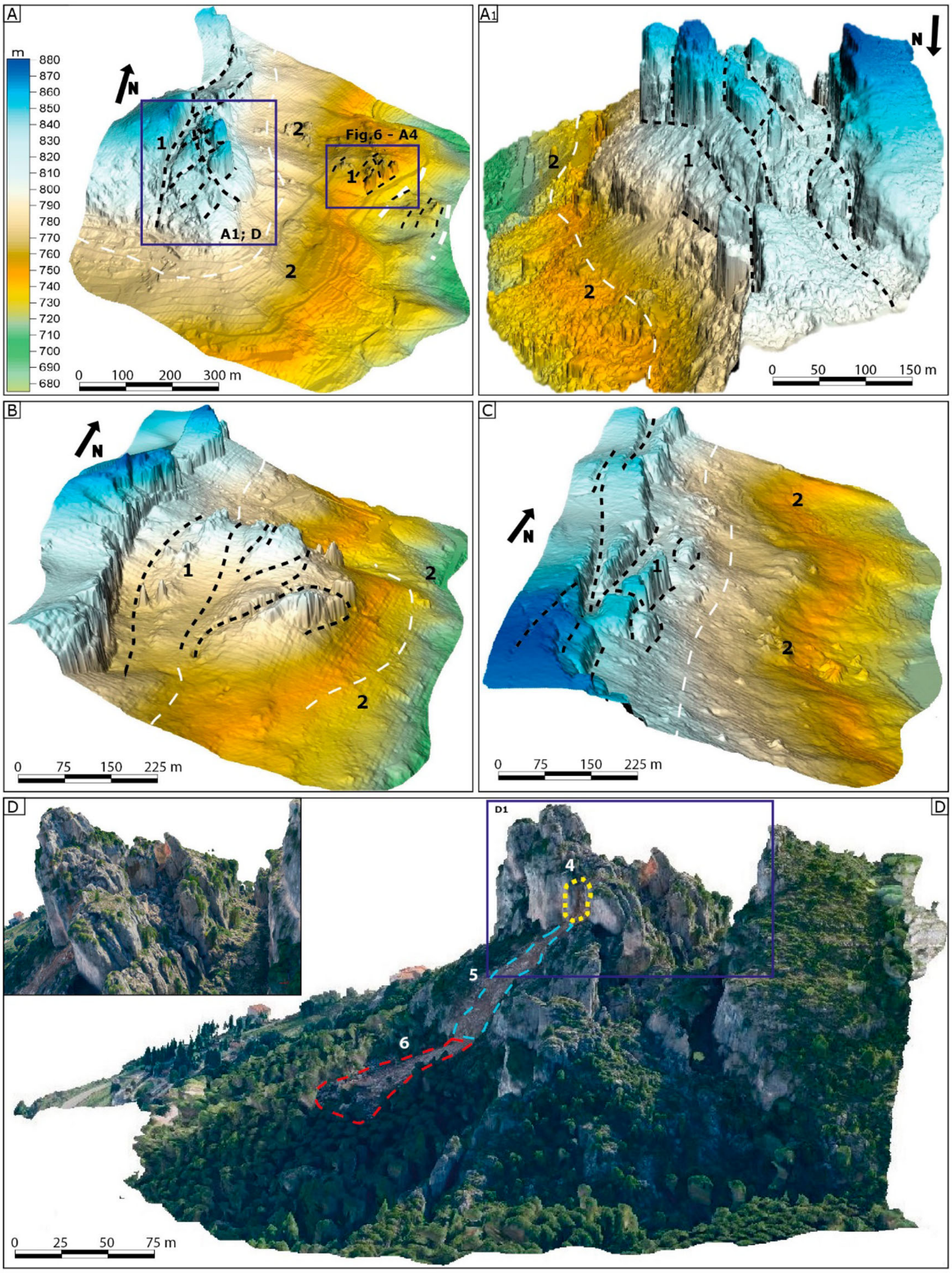

Figure 7. LiDAR 3D model of the DSGSD. (A1) Bruncu Pranedda. (B) Tisiddu Mountain. (C) Scala San Giorgio. (1) High fracturing area with active extensional trenches. (2) Collapse deposits of rock avalanches. The black dashed lines represent the major extensional trenches. White dashed lines represent the major stratigraphic discontinuity between marine Mesozoic sequence and the metamorphic basement. (D) UAV 3D model of Bruncu Pranedda. (4) Detachment niche. (5) Transit area. (6) Collapse deposits of rock avalanches.

major fracture; however, in the basement, it is ductile with a sub-horizontal movement. The basal sub-horizontal shear zone is primarily located in the Genna Selole Formation and in the summit altered metamorphites.

The second stage (Figure 8(2b,3)) is associated with the deformation pattern of the sackung type (Ambrosi & Crosta, 2006, 2011; Audemard et al., 2010; Bovis & Evans, 1996; Coquin et al., 2015; McCalpin & Irvine, 1995; Oppikofer et al., 2017; Soldati et al., 2004), which can be deduced from the partial sinking of the DSGSD body inside the Palaeozoic basement. This stage is the observable downslope of the plateau edges located in the parts of the Dorgali Formation

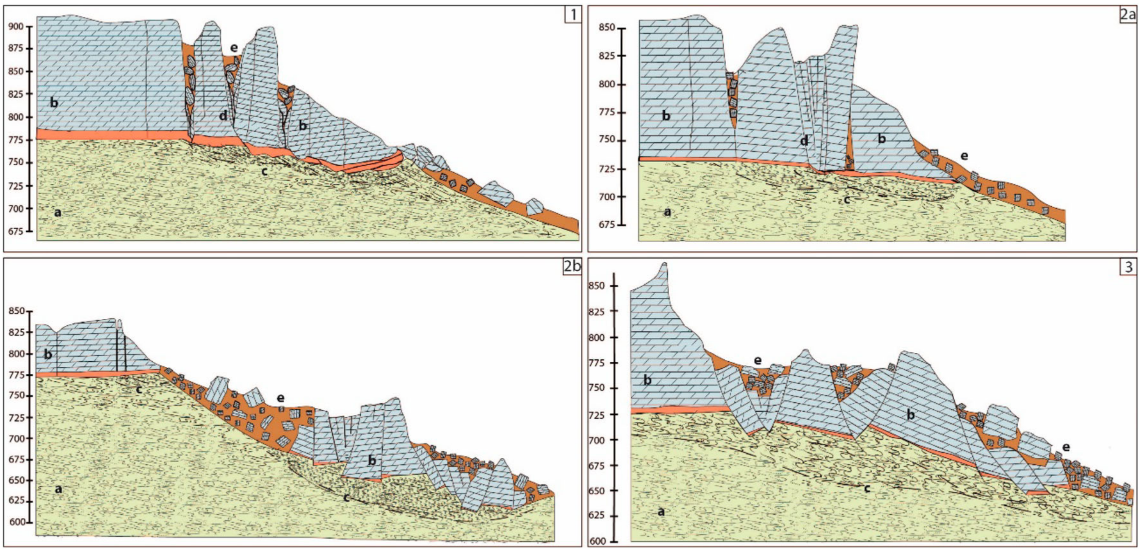

Figure 8. Interpretative geological cross-sections. (1) Scala San Giorgio, (2a) Bruncu Pranedda lateral spread; (2b) Bruncu Pranedda sackung; (3) Tisiddu Mountain sackung. (a) Metamorphic basement; Dorgali Formation over Genna Selole (orange). (c) Hypothetical shear zone, (d) active extensional trenches, (e) trench rockfall deposits.

tens of metres away from the original stratigraphic altitude. They are separated from the plateau by an extensive transit area characterised by the presence of slope deposits with limited outcrops of the Palaeozoic basement. This is an advanced stage assimilable at a sackung landslide and is associated with a major basal deformation that allows the movement of the bodies even for several hundreds of metres. The shear zone is located in the metamorphic basement with a sub-circular shape.

The third stage is the consequence of the collapse of the peripheral margins of DSGSDs and is manifested through rock avalanche deposits (Figure 6(D)). These deposits, comprising blocks with a size of several thousands of cubic metres, cover the most recent slope deposits and represent one of the major evidence for present movements of the DSGSDs. In fact, rock avalanche deposits have been found to exhibit sedimentological and geomorphological characteristics of a very recent event. The evidence of current activity is demonstrated by the detachment of a rock avalanche which occurred in November 2014, involving a total volume of rock more than 1500 m^3.

The type and evolutionary characteristics of rockfalls and rock avalanches represent high risk factors in some sectors of the inhabited centre below; a monitoring network is being created based on satellite and geotechnical technologies with the aim of developing an early warning system.

5. Conclusions

A kinematic model and geomorphological evolution characteristics of DSGSD in Sardinia were described for the first time in this study. The study highlighted an extremely young territory conformation, associated with the Neogene and Quaternary geodynamic events, implying a series of problems related to the slope process. The causes of the DSGSDs are associated with the structural characteristics of the area and the Neogene and Quaternary geomorphological evolution of the river valley associated with the recent uplift. In the main map, a comprehensive mapping of structural, karst, fluvial, and slope morphologies in Pardu and Ulassai valleys is presented.

The predisposing factors of DSGSDs can be identified in the following points:

1. The tectonic history of the slope with a passive influence has been caused by a major uplift associated with the Neogene and Quaternary geodynamic events. The upliftment has increased the erosion rates, thereby leading to the deepening of the valleys and detente of the slopes. The energy of the relief of the slopes is the decisive morphological element which initiates the DSGSDs; in the cases studied, it is higher than 650 m.

– Cenozoic tectonics have also conferred the structural conditions that predisposed the development of DSGSD, particularly in the Dorgali Formation. In fact, the major DSGSD trenches are evidently parallel to the major faults and primarily parallel to that of Pardu Valley in the NW–SE direction, on which the slope is also set

- The lithostratigraphic conditions are represented by the Mesozoic units on the foliated and altered metamorphic basement.

The initiation of rapid catastrophic processes such as rock avalanche is associated with the accelerations of DSGSDs. These accelerations are linked to seismic activities and extreme rainfall events. The latter cause the hydration of the rocks in the shear zones, thereby decreasing the geomechanical characteristics.

High-resolution topographic data and geological and geomorphological field surveys enabled the identification of three evolutionary stages of DSGSD.

- The first stage preceding the capture of the Rio Pardu by the Rio Pelau associated with the uplift and the Plio-Quaternary tectonics.
- The second phase associated with a major erosive activity following the capture of the Rio Pardu which triggered the oldest DSGSDs with sackung features.
- The present evolution of plateau edges through lateral spread DSGSDs and rock avalanches.

Software

The map was digitised using ESRI ArcGIS ® 10.6 software. UAV photogrammetry data were processed by Agisoft Metashape Professional ®. The digital terrain models were generated using the Global Mapper ® 21.0. Geological sections were created using Adobe Illustrator ® CC2015.

Acknowledgements

We thank the reviewers and editors for constructive comments during the reviews.

Disclosure statement

No potential conflict of interest was reported by the author(s).

Data availability statement

Raw data were generated at University of Cagliari (Italy). Derived data supporting the findings of this study are available on request from the corresponding author.

ORCID

Valentino Demurtas http://orcid.org/0000-0003-4187-0902
Paolo E. Orrù http://orcid.org/0000-0002-2394-3154
Giacomo Deiana http://orcid.org/0000-0002-7019-9153

References

Agliardi, F., Crosta, G., & Zanchi, A. (2001). Structural constraints on deepseated slope deformation kinematics. *Engineering Geology*, *59*(1–2), 83–102. https://doi.org/10.1016/S0013-7952(00)00066-1

Agliardi, F., Scuderi, M. M., Fusi, N., & Cristiano, C. (2020). Slow-to-fast transition of giant creeping rockslides modulated by undrained loading in basal shear zones. *Nature Communications*, *11*(1), 1352. https://doi.org/10.1038/s41467-020-15093-3

Ambrosi, C., & Crosta, G. B. (2006). Large sackung along major tectonic features in the central Italian Alps. *Engineering Geology*, *83*(1–3), 183–200. https://doi.org/10.1016/j.enggeo.2005.06.031

Ambrosi, C., & Crosta, G. B. (2011). Valley shape influence on deformation mechanisms of rock slopes. *Geological Society, London, Special Publications*, *351*(1), 215–233. https://doi.org/10.1144/SP351.12

Audemard, F., Beck, C., & Carrillo, E. (2010). Deep-seated gravitational slope deformations along the active Boconó Fault in the central portion of the Mérida Andes, western Venezuela. *Geomorphology*, *124*(3–4), 164–177. https://doi.org/10.1016/j.geomorph.2010.04.020

Bisci, C., Dramis, F., & Sorriso-Valvo, M. (1996). Rock flow (sackung). In R. Dikau, D. Brunsden, L. Schrott, & M.-L. Ibsen (Eds.), *Landslide Recognition: Identification, movement and causes* (pp. 150–160). John Wiley & Sons.

Bovis, M. J., & Evans, S. G. (1996). Extensive deformations of rock slopes in southern coast mountains, southwest British Columbia, Canada. *Engineering Geology*, *44*(1-4), 163–182. https://doi.org/10.1016/S0013-7952(96)00068-3

Carmignani, L., Carosi, R., Di Pisa, A., Gattiglio, G., Musumeci, G., Oggiano, G., & Pertusati, P. C. (1994). The Hercynian chain in Sardinia (Italy). *Geodinamica Acta*, *7*(1), 31–47. https://doi.org/10.1080/09853111.1994.11105257

Carmignani, L., Oggiano, G., Barca, S., Conti, P., Salvadori, I., Eltrudis, A., Funedda, A., & Pasci, S. (2001). *Geologia della Sardegna; Note Illustrative della Carta Geologica della Sardegna in scala 1:200.000. Memorie Descrittive della Carta Geologica d'Italia* (Vol. 60, 283pp). Servizio Geologico d'Italia.

Carmignani, L., Oggiano, G., Funedda, A., Conti, P., & Pasci, S. (2016). The geological map of Sardinia (Italy) at 1:250,000 scale. *Journal of Maps*, *12*(5), 826–835. https://doi.org/10.1080/17445647.2015.1084544

Carminati, E., & Doglioni, C. (2005). Mediterranean tectonics. In R. Selley, R. Cocks, & I. Plimer (Eds.), *Encyclopedia of geology* (pp. 135–146). Elsevier.

Casula, G., Cherchi, A., Montadert, L., Murru, M., & Sarria, E. (2001). The cenozoic graben system of Sardinia (Italy): Geodynamic evolution from new seismic and field data. *Marine and Petroleum Geology*, *18*(7), 863–888. https://doi.org/10.1016/S0264-8172(01)00023-X

Cherchi, A., & Montadert, L. (1982). Oligo-Miocene rift of Sardinia and the early history of the Western Mediterranean Basin. *Nature*, *298*(5876), 736–739. https://doi.org/10.1038/298736a0

Chigira, M. (1992). Long-term gravitational deformation of rocks by mass rock creep. *Engineering Geology*, *32*(3), 157–184. https://doi.org/10.1016/0013-7952(92)90043-X

Cimini, G. B., Marchetti, A., & Silvestri, M. (2016). *L'esperimento Sardinia passive array (spa): acquisizione dati sismici per lo studio della geodinamica e della sismotettonica dell'area mediterranea*. INGV (Istituto Nazionale di Geofisica e Vulcanologia, Centro Nazionale Terremoti).

Clapuyt, F., Vanacker, V., & Oost, K. V. (2016). Reproducibility of UAV-based earth topography reconstructions based on structure-from-motion algorithms. *Geomorphology*, *260*, 4–15. https://doi.org/10.1016/j.geomorph.2015.05.011

Coquin, J., Mercier, D., Bourgeois, O., Cossart, E., & Decaulne, A. (2015). Gravitational spreading of mountain ridges coeval with late Weichselian deglaciation: Impact on glacial landscapes in Tröllaskagi, northern Iceland.

Quaternary Science Reviews, *107*, 197–213. https://doi.org/10.1016/j.quascirev.2014.10.023
Costamagna, L. G. (2015). Middle Jurassic continental to marine transition in an extensional tectonics context: The Genna Selole Fm depositional system in the Tacchi area (central sardinia. Italy). *Geological Journal*, *51*(5), 722–736. https://doi.org/10.1002/gj.2680
Costamagna, L. G., & Barca, S. (2004). Stratigraphy, facies analysis, paleogeography and regional framework of the Jurssic succession of the "tacchi" area (Middle-Eastern Sardinia). *Bollettino della Societa Geologica Italiana*, *123*(3), 477–495.
Costamagna, L. G., Kustatscher, E., Scanu, G. G., Del Rio, M., Pittau, P., & Van Konijnenburg-van Cittert, J. H. A. (2018). A palaeoenvironmental reconstruction of the Middle Jurassic of Sardinia (Italy) based on integrated palaeobotanical, palynological and lithofacies data assessment. *Palaeobiodiversity and Palaeoenvironments*, *98*(1), 111–138. https://doi.org/10.1007/s12549-017-0306-z
Crosta, G. B., & Agliardi, F. (2003). Failure forescast for large rock slides by surface displacement measurements. *Canadian Geotechnical Journal*, *40*(1), 176–191. https://doi.org/10.1139/t02-085
Crosta, G. B., Frattini, P., & Agliardi, F. (2013). Deep seated gravitational slope deformations in the European Alps. *Tectonophysics*, *605*, 13–33. https://doi.org/10.1016/j.tecto.2013.04.028
Crosta, G. B., & Zanchi, A. (2000). Deep-seated slope deformations. Huge, extraordinary, enigmatic phenomena. In E. Bromhead, N. Dixon, & M. Ibsen (Eds.), *Landslides in research, theory and practice* (pp. 351–358). Thomas Telford.
Cruden, D. M., & Varnes, D. J. (1996). *Landslide Types and Processes*. Transportation Research Board, U.S. National Academy of Sciences, Special Report (Vol. 247, pp. 36–75).
Deiana, G., Lecca, L., Melis, R. T., Soldati, M., Demurtas, V., & Orrù, P. E. (2021). Submarine Geomorphology of the southwestern Sardinian continental shelf (Mediterranean Sea): Insights into the last glacial maximum sea-level changes and related environments. *Water*, *13*(2), 155. https://doi.org/10.3390/w13020155
Delgado, J., Vicente, F., García-Tortosa, F., Alfaro, P., Estévez, A., Lopez-Sanchez, J. M., Tomás, R., & Mallorquí, J. J. (2011). A deep seated compound rotational rock slide and rock spread in SE Spain: Structural control and DInSAR monitoring. *Geomorphology*, *129*(3–4), 252–262. https://doi.org/10.1016/j.geomorph.2011.02.019
Devoto, S., Macovaz, V., Mantovani, M., Soldati, M., & Furlani, S. (2020). Advantages of using UAV digital photogrammetry in the study of slow-moving coastal landslides. *Remote Sensing*, *12*(21), 3566. https://doi.org/10.3390/rs12213566
De Waele, J., Di Gregorio, F., Follesa, R., & Piras, G. (2005). Geosites and landscape evolution of the "tacchi": an example from central-east Sardinia. *Il Quaternario*, *18*(1), 211–220.
De Waele, J., Ferrarese, F., Granger, D., & Sauro, F. (2012). Landscape evolution in the Tacchi area (central-east Sardinia, Italy) based on karst and fluvial morphology and age of cave sediments. *Geografia Fisica e Dinamica Quaternaria*, *35*, 119–127. 10.4461/GFDQ.2012.35.11
Dieni, I., Fischer, J. C., Massari, F., Salard-Cheboldaeff, M., & Vozenin-Serra, C. (1983). La succession de Genna Selole (Baunei) dans le cadre de la paléogéographie mésojurassique de la Sardaigne orientale. *Memorie della Società Geologica Italiana*, *36*, 117–148.
Dramis, F., Farabollini, P., Gentili, B., & Pambianchi, G. (2002, September 21–27). Neotectonics and large scale gravitational phenomena in the Umbria –Marche Apennines, Italy. In V. Comerci, N. D'Agostino, G. Fubelli, P. Molin, & T. Piacentini (Eds.), *Seismically induced ground ruptures and large scale mass movements, Field excursion and Meeting Atti APAT 4/2002* (Vol. 21, pp. 17–30).
Dramis, F., & Sorriso-Valvo, M. (1994). Deep-seated gravitational slope deformations, related landslides and tectonics. *Engineering Geology*, *38*(3–4), 231–243. https://doi.org/10.1016/0013-7952(94)90040-X
Eker, R., & Aydın, A. (2021). Long-term retrospective investigation of a large, deep-seated, and slow-moving landslide using InSAR time series, historical aerial photographs, and UAV data: The case of Devrek landslide (NW Turkey). *Catena*, *196*. https://doi.org/10.1016/j.catena.2020.104895
Elter, F. M., Corsi, B., Cricca, P., & Muzio, G. (2004). The south-western Alpine foreland: Correlation between two sectors of the Variscan chain belonging to "stable Europe": Sardinia (Italy) Corsica and Maures Massif (South-Eastern France). *Geodinamica Acta*, *17*(1), 31–40. https://doi.org/10.3166/ga.17.31-40
Elter, F. M., Padovano, M., & Kraus, R. K. (2010). The emplacement of Variscan HTmetamorphic rocks linked to the interaction between Gondwana and Laurussia: Structural constraints in NE Sardinia (Italy). *Terra Nova*, *22*(5), 369–377. https://doi.org/10.1111/j.1365-3121.2010.00959.x
Ferranti, L., Oldow, J. S., D'Argenio, B., Catalano, R., Lewis, D., Marsella, E., Avellone, G., Maschio, L., Pappone, G., Pepe, F., & Sulli, A. (2008). Active deformation in Southern Italy, Sicily and southern Sardinia from GPS velocities of the Peri-Tyrrhenian Geodetic Array (PTGA). *Bollettino della Società Geologica Italiana*, *127*(2), 299–316.
Fioraso, G. (2017). Impact of massive deep-seated rock slope failures on mountain valley morphology in the northern Cottian Alps (NW Italy). *Journal of Maps*, *13*(2), 575–587. https://doi.org/10.1080/17445647.2017.1342211
Fleurant, C., Tucker, G. E., & Viles, H. A. (2008). A model of cockpit karst landscape, Jamaica. In *Géomorphologie: relief, processus, environnement, Groupe français de géomorphologie (GFG)* (pp. 3–14).
Frattini, P., Crosta, G. B., Rossini, M., & Allievi, J. (2018). Activity and kinematic behaviour of deep-seated landslides from PS-InSAR displacement rate measurements. *Landslides*, *15*(6), 1053–1070. https://doi.org/10.1007/s10346-017-0940-6
Gattacceca, J., Deino, A., Rizzo, R., Jones, D. S., Henry, B., Beaudoin, B., & Vadeboin, F. (2007). Miocene rotation of Sardinia: New paleomagnetic and geochronological constraints and geodynamic implications. *Earth and Planetary Science Letters*, *258*(3-4), 359–377. https://doi.org/10.1016/j.epsl.2007.02.003
GNGFG. (1994). Proposta di legenda geomorfologica ad indirizzo applicativo. *Geografia Fisica e Dinamica Quaternaria*, *16*(2), 129–152.
Gueguen, E., Doglioni, C., & Fernandez, M. (1997). Lithospheric boudinage in the Western Mediterranean back-arc basin. *Terra Nova*, *9*(4), 184–187. https://doi.org/10.1046/j.1365-3121.1997.d01-28.x

Gutiérrez-Santolalla, F., Acosta, E., Ríos, S., Guerrero, J., & Lucha, P. (2005). Geomorphology and geochronology of sackung features (uphill-facing scarps) in the central spanish pyrenees. *Geomorphology*, *69*(1–4), 298–314. https://doi.org/10.1016/j.geomorph.2005.01.012

INGV. (2021). INGV special, the earthquakes of 2020 in Italy.

ISPRA. (2007). *Guida alla rappresentazione cartografica della Carta Geomorfologica d'Italia in scala 1:50,000. Quaderni Serie III del Servizio Geologico Nazionale*.

ISPRA & AIGEO. (2018). *Aggiornamento ed integrazione delle linee guida della Carta Geomorfologica d'Italia in scala 1:50,000. Quaderni Serie III del Servizio Geologico Nazionale*.

Jahn, A. (1964). Slope morphological feature resulting from gravitation. *Zeitschrift für Geomorphologie*(Suppl. 5), 59–72.

Liang, F., & Xu, B. (2014). Discrimination of tower-, cockpit-, and non-karst landforms in Guilin, Southern China, based on morphometric characteristics. *Geomorphology*, *204*, 42–48. https://doi.org/10.1016/j.geomorph.2013.07.026

Lustrino, M., Melluso, L., & Morra, V. (2007). The geochemical peculiarity of Plio-Quaternary volcanic rocks of Sardinia in the circum-Mediterranean area. *Geological Society of America*, *418*, 277–301. https://doi.org/10.1130/2007.2418(14)

Mantovani, M., Devoto, S., Piacentini, D., Prampolini, M., Soldati, M., & Pasuto, A. (2016). Advanced SAR interferometric analysis to support geomorphological interpretation of slow-moving coastal landslides (Malta, Mediterranean Sea). *Remote Sensing*, *8*(6), 443. https://doi.org/10.3390/rs8060443

Mariani, G. S., & Zerboni, A. (2020). Surface geomorphological features of deep-seated gravitational slope deformations: A look to the role of lithostructure (N Apennines, Italy). *Geosciences*, *10*(9), 334. https://doi.org/10.3390/geosciences10090334

Marini, A., & Ulzega, A. (1977). Osservazioni geomorfologiche sul tacco di ulassai. *Rendiconti Seminario Facoltà Scienze Università di Cagliari*, *47*(1–2), 192–208.

Marini, C. (1984). Le concentrazioni residuali post-erciniche di Fe dell'Ogliastra (Sardegna orientale): contesto geologico e dati mineralogici. *Rendiconti della Societa Italiana di Mineralogia e Petrologia*, *39*, 229–238.

Maxia, C., Ulzega, A., & Marini, C. (1973). Studio idrogeologico dei dissesti nel bacino del rio Pardu (Sardegna centro-orientale). *Pubblicazione dell'Istituto di Geologia, Paleontologia e Geografia Fisica*, *121*(12), 9.

McCalpin, J., & Irvine, J. R. (1995). Sackungen at the Aspen Highlands Ski area, Pitkin County, Colorado. *Environmental & Engineering Geoscience*, *I*(3), 277–290. https://doi.org/10.2113/gseegeosci.I.3.277

Meloni, M. A., Oggiano, G., Funedda, A., Pistis, M., & Linnemann, U. (2017). Tectonics, ore bodies, and gamma-ray logging of the Variscan basement, southern Gennargentu massif (central Sardinia, Italy). *Journal of Maps*, *13*(2), 196–206. https://doi.org/10.1080/17445647.2017.1287601.

Miccadei, E., Orrù, P., Piacentini, T., Mascioli, F., & Puliga, G. (2012). Geomorphological map of the Tremiti Islands (Puglia, Southern Adriatic Sea, Italy), scale 1:15,000. *Journal of Maps*, *8*(1), 74–87. https://doi.org/10.1080/17445647.2012.668765

Nemčok, A. (1972). Gravitational slope deformation in high mountains. In *Proceedings of the 24th International Geology Congress*, Montreal, Sect. 13 (pp. 132–141).

Novellino, A., Cesarano, M., Cappelletti, P., Di Martire, D., Di Napoli, M., Ramondini, M., Sowter, A., & Calcaterra, D. (2021). Slow-moving landslide risk assessment combining machine learning and InSAR techniques. *Catena*, *203*. https://doi.org/10.1016/j.catena.2021.105317

Oggiano, G., Funedda, A., Carmignani, L., & Pasci, S. (2009). The Sardinia-Corsica microplate and its role in the northern Apennine geodynamics: New insights from the tertiary intraplate strike-slip tectonics of Sardinia. *Italian Journal of Geosciences*, *128*(2), 527–541. https://doi.org/10.3301/IJG.2009.128.2.527

Oppikofer, T., Saintot, A., Hermanns, R., Böhme, M., Scheiber, T., Gosse, J., & Dreiås, G. (2017). From incipient slope instability through slope deformation to catastrophic failure—Different stages of failure development on the Ivasnasen and Vollan rock slopes (western Norway). *Geomorphology*, *289*, 96–116. https://doi.org/10.1016/j.geomorph.2017.03.015

Ostermann, M., & Sanders, D. (2017). The Benner pass rock avalanche cluster suggests a close relation between long-term slope deformation (DSGSDs and translational rock slides) and catastrophic failure. *Geomorphology*, *289*, 44–59. https://doi.org/10.1016/j.geomorph.2016.12.018

Palomba, M., & Ulzega, A. (1984). Geomorfologia dei depositi quaternari del Rio Quirra e della piattaforma continentale antistante (Sardegna Orientale). *Rendiconti Saminario Facoltà Scienze. Università Cagliari*, *54*(2).

Pánek, T., & Klimeš, J. (2016). Temporal behavior of deep-seated gravitational slope deformations: A review. *Earth-Science Reviews*, *156*, 14–38. https://doi.org/10.1016/j.earscirev.2016.02.007

Pasuto, A., & Soldati, M. (1996). Lateral spreading. In R. Dikau, D. Brunsden, L. Schrott, & M.-L. Ibsen (Eds.), *Landslide recognition: Identification, movement and causes* (pp. 122–136). Wiley.

Pertusati, P. C., Sarria, E., Cherchi, G. P., Carmignani, L., Barca, S., Benedetti, M., Chighine, G., Cincotti, E., & Oggiano, G. (continental area). Ulzega, A., Orrù, P.E., & Pintus, C. (marine area) (2002). *Geological Map of Italty. Scale 1:50.000*. Scheet 541 "Jerzu" – ISPRA-Servizio Geologico Nazionale.

Peternal, T., Kumelj, S., Ostir, K., & Komac, M. (2017). Monitoring the Potoška planina landslide (NW Slovenia) using UAV photogrammetry and tachymetric measurements. *Landslides*, *14*(1), 395–406. https://doi.org/10.1007/s10346-016-0759-6

Radbruch-Hall, D. (1978). Gravitational creep of rock masses on slopes. In B. Voight (Ed.), *Rockslides and avalanches – Natural phenomena: Developments in geotechnical engineering* (Vol. 14, pp. 607–658). Elsevier.

Radbruch-Hall, D., Varnes, D. J., & Savage, W. Z. (1976). Gravitational spreading of steep-sided ridges ("sackung") in western United States. *IAEG Bulletin*, *14*, 23–35. https://doi.org/10.1007/BF02634754

Smith, M. J., Paron, P., & Griffiths, J. (2011). *Geomorphological mapping, methods and applications: Vol. 15. Developments in earth surface processes*. Elsevier Science.

Soldati, M. (2013). Deep-seated gravitational slope deformation. In P. T. Bobrowsky (Ed.), *Encyclopedia of natural hazards. Encyclopedia of earth sciences series*. Springer.

Soldati, M., Corsini, A., & Pasuto, A. (2004). Landslides and climate change in the Italian dolomites since the late glacial. *Catena*, *55*(2), 141–161. https://doi.org/10.1016/S0341-8162(03)00113-9

Taramelli, A., & Melelli, L. (2008). Map of deep seated gravitational slope deformations susceptibility in central Italy derived from SRTM DEM and spectral mixing analysis of the landsat ETM+ data. *International Journal of Remote Sensing*, *30*(2), 357–387. https://doi.org/10.1080/01431160802339449

Ulzega, A., & Marini, A. (1973). L'évolution des versants dans la vallée du Rio Pardu (Sardaigne centre-orientale). *Zeitschrift fur Geomorphologie*, *21*(4), 466–474.

Ulzega, A., Orrù, P. E., & Pintus, C. (marine area). Pertusati, P. C., Sarria, E., Cherchi, G. P., Carmignani, L., Barca, S., Benedetti, M., Chighine, G., Cincotti, E., & Oggiano, G. (continental area). (2002). *Geological Map of Italty. Scale 1:50.000*. Scheet 541 "Jerzu" – ISPRA- Servizio Geologico Nazionale.

Vai, G. B., & Cocozza, T. (1974). Il "postgotlandiano" sardo, unità sinorogenica ercinica. *Bollettino della Società geologica italiana*, *93*, 61–72.

Valkaniotis, S., Papathanassiou, G., & Ganas, A. (2018). Mapping an earthquake-induced landslide based on UAV imagery; case study of the 2015 Okeanos landslide, Lefkada, Greece. *Engineering Geology*, *245*, 141–152. https://doi.org/10.1016/j.enggeo.2018.08.010

Waltham, T. (2008). Fengcong, fenglin, cone karst and tower karst Cave and Karst. *Science*, *35*(3), 77–88.

Zaruba, Q., & Mencl, V. (1982). *Landslides and their control: Development in geotechnical engineering*. Elsevier, 324p.

Zischinsky, U. (1966). On the deformation of high slopes. In *Proceedings of the 1st Conference International Society for Rock Mechanics*, Lisbon, Sect 2 (pp. 179–185).

ZischinskY, U. (1969). Über Sackungen. *Rock Mechanics*, *1* (1), 30–52. doi:10.1007/BF01247356